NASA TECHNICAL NOTE

NASA TN D-6398

NASA TN D-6398

FLIGHT-DETERMINED ACCELERATION AND CLIMB PERFORMANCE OF AN F-104G AIRPLANE FOR USE IN AN OPTIMUM-FLIGHT-PATH COMPUTER PROGRAM

by Robert T. Marshall

Flight Research Center
Edwards, Calif. 93523

NATIONAL AERONAUTICS AND SPACE ADMINISTRATION • WASHINGTON, D. C. • JUNE 1971

1. Report No.	2. Government Accession No.	3. Recipient's Catalog No.
NASA TN D-6398		

4. Title and Subtitle	5. Report Date
FLIGHT-DETERMINED ACCELERATION AND CLIMB PERFORMANCE OF AN F-104G AIRPLANE FOR USE IN AN OPTIMUM-FLIGHT-PATH COMPUTER PROGRAM	June 1971
	6. Performing Organization Code
7. Author(s)	8. Performing Organization Report No.
Robert T. Marshall	H-636
9. Performing Organization Name and Address	10. Work Unit No.
NASA Flight Research Center P. O. Box 273 Edwards, California 93523	125-17-04-04-24
	11. Contract or Grant No.
12. Sponsoring Agency Name and Address	13. Type of Report and Period Covered
National Aeronautics and Space Administration Washington, D. C. 20546	Technical Note
	14. Sponsoring Agency Code

15. Supplementary Notes

16. Abstract

A flight-test investigation was conducted to determine the standard-day performance characteristics (excess thrust, fuel flow, and climb potential) at maximum afterburner power for an F-104G airplane. The tests were conducted at Mach numbers from 0.5 to 2.0 and at altitudes from 5000 feet (1524 meters) to 50,000 feet (15,240 meters).

The standard-day excess thrust and fuel-flow data obtained from the investigation were used to define a computer model of the performance of the test airplane. In addition, the climb-potential (specific excess power) data obtained from the flight tests were compared with the available predicted climb-potential data. From the comparisons, it was found that the predicted data for the "average" F-104G airplane did not represent the performance of the test airplane as accurately as required for the computation of meaningful flight trajectories. Therefore, to compute meaningful flight trajectories for the test airplane, the flight-derived model should be used.

17. Key Words (Suggested by Author(s))	18. Distribution Statement
Performance F-104G airplane Trajectory optimization	Unclassified - Unlimited

19. Security Classif. (of this report)	20. Security Classif. (of this page)	21. No. of Pages	22. Price*
Unclassified	Unclassified	36	$3.00

*For sale by the National Technical Information Service, Springfield, Virginia 22151

FLIGHT-DETERMINED ACCELERATION AND CLIMB PERFORMANCE OF AN F-104G AIRPLANE FOR USE IN AN OPTIMUM-FLIGHT-PATH COMPUTER PROGRAM

By Robert T. Marshall
Flight Research Center

INTRODUCTION

With the expanded flight envelopes of today's aircraft and the performance penalties associated with nonoptimum flight paths, it is desirable to determine the minimum-time-to-climb or minimum-fuel-consumed flight paths, or both, for an aircraft. At present, sophisticated, ground-base computer programs are used to obtain the optimum flight path between any two points within the flight envelope of an aircraft (refs. 1 to 6). However, the use of these optimization techniques is limited in that they require large ground-base computers and long computational times and use model atmospheres that do not always adequately represent the flight environment. In addition, a schedule for each optimum flight path to be flown must be presented to the pilot before each flight.

With the recent development of improved computational techniques, such as dynamic programing methods (ref. 7), and the increased capability of airborne digital computers, the technology now exists to overcome the noted limitations. These developments make possible the approximate real-time airborne computation and display of an optimum flight path which applies to the actual atmospheric conditions encountered in flight. However, for the computation of meaningful flight trajectories, an accurate performance model, in terms of the climb and acceleration capabilities of the aircraft, is required together with a means of adjusting the performance model for variations in atmospheric conditions. It is essential that these two requirements be met, or the capability to compute a flight path enroute will be of little use to the pilot.

This report presents the results of a flight-test program conducted at the NASA Flight Research Center to determine the standard-day performance characteristics of the F-104G, S/N 56-0790, airplane. These characteristics will be used to investigate the utilization of an airborne system for the real-time computation of an optimum flight path. This test program was conducted because it was believed that the available predicted data (ref. 8), which are for an "average" or typical F-104G airplane, would not represent the actual performance of the test airplane to the degree of accuracy required for the computation of meaningful flight trajectories.

The predicted and measured climb and acceleration capability of the test airplane are compared. In addition, the correction procedures that can be used to adjust the standard-day data to whatever flight conditions encountered are presented.

SYMBOLS

The standard-day performance data defined in this report were computed in the U. S. Customary System of Units. The equivalent values in the International System of Units (SI) are given in parentheses. Factors relating the two systems are presented in reference 9.

C_D	drag coefficient, $\frac{\text{Drag}}{qS}$
$\frac{\Delta C_D}{\Delta C_L^{\ 2}}$	drag-due-to-lift parameter
C_L	lift coefficient, $\frac{\text{Lift}}{qS}$
D	total aircraft drag, lb (N)
FC	fuel used, counts
FD	fuel density, lb/gal (kg/m^3)
F_n	net thrust, lb (N)
$F_{n,ex}$	excess thrust, F_n - D, lb (N)
FU	fuel used, lb (kg)
g	acceleration due to gravity, 32.2 ft/sec^2 (9.8 m/sec^2)
He	instantaneous specific energy, ft (m)
h	pressure altitude, ft (m)
Δh_{pc}	altitude position-error correction, ft (m)

K	calibration constant
M	Mach number
ΔM_{pc}	Mach number position-error correction
p_a	ambient pressure, in. Hg (N/m^2)
p_{t_2}	compressor inlet total pressure, in. Hg (N/m^2)
q	dynamic pressure, lb/ft^2 (N/m^2)
R/C	instantaneous climb potential, ft/min (m/sec)
S	wing reference area, ft^2 (m^2)
T_a	ambient temperature, °F (°C) or °C (°K)
T_f	fuel temperature, °F (°C) or °C (°K)
T_{tot}	total temperature, °F (°C) or °C (°K)
t	time, sec
V	velocity, knots or ft/sec (m/sec)
W	airplane gross weight, lb (kg)
W_f	fuel flow, lb/sec (kg/sec)
$\Delta(\ )$	change in specified parameter

δ_{t_2}	compressor inlet total-pressure ratio, $\frac{p_{t_2}}{29.92}$ $\left(\frac{p_{t_2}}{101,320}\right)$

Subscripts:

ab	afterburner
e	main engine
es	engine start
i	indicated
ic	instrument corrected value
id	induced drag
s	standard-day condition
T	true value
t	test-day condition
tot	total value
w	weight correction

AIRPLANE DESCRIPTION

The performance flight-test program was conducted with the F-104G prototype airplane, S/N 56-0790 (fig. 1), a modified F-104A airplane. Although the airplane is a modified F-104A airplane, the basic external dimensions, surface areas, and control systems are those of an F-104G airplane. A three view drawing of the F-104G airplane is shown in figure 2, and pertinent physical characteristics are given in table 1. The airplane is described in detail in reference 8.

The airplane is powered by a General Electric J79-GE-11A engine, a high-pressure-ratio, single-rotor, afterburning turbojet engine. The entire flight-test program was conducted with one engine. The engine required no retrimming during the program. A detailed description and minimum performance characteristics of the engine are included in reference 10.

INSTRUMENTATION

The instrumentation installed in the test airplane for this program included a photopanel, a self-recording three-component accelerometer, a test nose boom, and two precision volumetric flow meters. The photopanel shown in figure 3 was installed in the nose compartment and was equipped with a 16-millimeter camera which was pulsed at 1 frame per second for all data runs. The photopanel was also equipped with a time-code generator which was set prior to each flight to give the time of day. The parameters displayed on the photopanel and the instrument operating ranges and resolutions were as follows:

Parameter	Range	Resolution
Indicated airspeed, knots	0 to 800	±0.5
Indicated pressure altitude, ft (m)	0 to 60,000 (0 to 18,288)	±5 (±1.52)
Angle of attack, deg (rad)	-5 to 20 (-0.087 to 0.349)	±0.5 (±0.0087)
Engine rpm, percent	0 to 100	±1
Exhaust gas temperature, °C (°K)	0 to 1000 (273.16 to 1273.16)	±5 (±5)
Fuel used (engine), counts[1]	0 to 9999.9	±0.1
Fuel used (afterburner), counts[2]	0 to 9999.9	±0.1
Fuel temperature (engine), °C (°K)	0 to 200 (273.16 to 473.16)	±2.5 (±2.5)
Fuel temperature (afterburner), °C (°K)	0 to 250 (273.16 to 523.16)	±2.5 (±2.5)
Throttle angle, deg (rad)	0 to 100 (0 to 1.745)	±0.5 (±0.0087)
Outside air stagnation temperature, °C (°K)	-30 to 150 (243.16 to 423.16)	±1 (±1)
Horizontal stabilizer position, deg (rad)	5 to -17 (0.087 to 0.297)	±0.5 (±0.0087)
Time	----------	Hours, minutes, seconds

[1] 1 count = 5.67 gal (0.02146 m^3)

[2] 1 count = 12.57 gal (0.04758 m^3)

The self-recording three-component accelerometer was installed as close to the airplane center of gravity as possible. The recording unit had a film speed of 0.75 in./sec (0.019 m/sec). The ranges and resolutions of the three accelerations are tabulated on the following page. For correlation, the photopanel time code was recorded as a pulse type of signal (IRIG E format) on the film.

Parameter	Range	Resolution
Longitudinal acceleration, g	±1	±0.005
Normal acceleration, g	-1 to 4	±0.01
Lateral acceleration, g	±1	±0.005
Time	- - - -	Hours, minutes, seconds

The test-day ambient temperature at altitude was obtained from a weather balloon. The balloon passed through the test altitudes within 90 minutes of the actual flight time and within 50 miles (80.5 kilometers) of the actual flight path. The accuracy of these temperature data is ±2° C (±2° K).

A test nose boom with a standard NACA pitot-static probe (ref. 11) was installed on the airplane.

STATIC-PRESSURE POSITION-ERROR CALIBRATION

Before the performance data were analyzed, it was necessary to obtain a position-error calibration for the test airplane, because the static-pressure source during flight testing is usually not in a position at which the pressure is ambient. Therefore, corrections are required to determine the true (ambient) pressure so that true Mach number and true pressure altitude may be computed.

The position-error calibration was determined from tower flyby data and from FPS-16 precision radar tracking data obtained during accelerations and decelerations at constant altitudes. For these data runs an ambient pressure was required for comparison with the measured pressure at the static source. For the tower flyby runs a precise barometer located in an adjacent tower provided the true ambient pressure, then theoretical adjustments were made for the small differences in elevation between the airplane and the tower. For the acceleration and deceleration runs, a combination of precision FPS-16 radar tracking data and radiosonde balloon data was used to compute the correct ambient pressure. Figures 4 and 5 are the position-error calibration curves used to determine the true Mach number and true pressure altitude from the indicated measurements.

TESTS

Nonsteady-state (dynamic) performance test methods were used to determine the performance of the test airplane. The test data were obtained for level-flight accelerations and for constant-Mach-number climbs at maximum power and at a constant heading. The speed and altitude information obtained was used to determine the total energy of the airplane, which is the sum of the potential and kinetic energy at a given point in the flight envelope. The rate of change of the total energy per unit time for the airplane is a measure of the climb potential (specific excess power) of the vehicle.

The test conditions selected for the level-flight accelerations and the constant-Mach-number climbs are presented in table 2. The flight-test conditions were selected to provide performance data for most of the operating envelope of the test airplane. The airplane was flown in a clean configuration (landing gear and flaps retracted and no external stores) for all test conditions. In addition, the airplane's center of gravity was allowed to travel along a normal schedule, because the range of this variable for the tests was such that it would not affect the results.

DATA ANALYSIS

The flight-test performance data of an aircraft are easily obtained from the measured test-day data, but this information has little meaning when parameters from flights flown on different days are compared. To avoid this problem, it is necessary to reduce the flight-test results to those which would have been obtained if the flights were flown under ideal standard-day conditions.

Specific-energy analysis methods (refs. 12 to 14) were used to compute the test-day performance data and to standardize the data to an airplane gross weight of 18,000 pounds (8165 kilograms) and the 1962 U. S. Standard Atmosphere. The data analysis methods used for computing and applying the standardization correction factors are discussed in detail in the appendix. The analysis methods are general (in a mathematical sense), in that they can be applied to correct a given set of data to any appropriate set of reference conditions. It therefore follows that these analysis methods can be used equally well to calculate the performance of the airplane for any given nonstandard day from the normalized standard-day data, and, similarly, these methods provide adjustments which compensate for variations in weight from a standard weight.

RESULTS AND DISCUSSION

Excess Thrust

The standard-day variation of excess thrust with increasing Mach number for the test airplane as determined from the level-flight acceleration data is presented in figures 6(a) to 6(e) for altitudes of 10,000 feet (3048 meters) to 50,000 feet (15,240 meters) at 10,000-foot (3048-meter) intervals. Two acceleration runs (A and B) were flown at each altitude with different atmospheric conditions and airplane gross weights for each run.

To provide some insight into the excess-thrust data, a schematic of typical F-104G thrust and drag curves (ref. 15) is presented in figure 7 for the test altitudes at a constant airplane weight. From figure 7, the qualitative relationship between the thrust, F_n, drag, D, and therefore the excess thrust, $F_n - D$, can be seen as a function of Mach number and altitude.

Figure 7 shows that in level flight at subsonic speeds the thrust increases almost linearly with Mach number. As indicated by the crosshatched regions, as the speed

increases in the subsonic region, the excess thrust increases from some initial level to a maximum and then rapidly decreases as the transonic drag rise is encountered. The flight-test data in figures 6(a) to 6(d), as expected, clearly show this subsonic variation of excess thrust with Mach number.

At supersonic speeds, as shown in figure 7, the variation of excess thrust with increasing Mach number is dependent on the altitude at which the airplane is operating. For example, the excess thrust decreases as the Mach number increases above 1.0 at an altitude of 10,000 feet (3048 meters). Conversely, excess thrust increases with supersonic Mach numbers at an altitude of 50,000 feet (15,240 meters). The flight-test data in figures 6(a) to 6(e) show the variation of excess thrust with altitude and supersonic Mach number.

For altitudes of 20,000 feet (6096 meters) and greater, the thrust increases sharply when a J79 engine operating characteristic known as "T_2 reset" is encountered, as illustrated in figure 7. T_2 reset advances the engine rpm by 4 percent to improve the engine stall margin at compressor inlet temperatures greater than 194° F (90° C). This advance in rpm also increases the maximum available thrust of the engine, which in turn accounts for an increase in the excess thrust of the airplane, as shown. T_2 reset is discussed in detail in reference 15.

The effect of T_2 reset on the data of this study can be seen in figures 6(b), 6(c), and 6(d) as an increase in the excess thrust at Mach numbers of 1.50, 1.72, and 1.95, respectively. Although T_2 reset would ordinarily be expected to occur as indicated in figure 7 for an altitude of 50,000 feet (15,240 meters), figure 6(e) does not show an increase in excess thrust due to T_2 reset, because the colder-than-standard ambient temperatures encountered during the level accelerations at this altitude caused a delay in the activation of T_2 reset until Mach 2.0.

Fuel Flow

Figure 8 presents the standard-day, maximum-power fuel-flow rates for the J79-GE-11A engine installed in the test airplane. As expected, the fuel flow increases with increasing Mach number for a given altitude and decreases with increasing altitude for a given Mach number. When T_2 reset is encountered, the fuel-flow rate increases rapidly for Mach numbers greater than 1.50, 1.72, and 1.95 at altitudes of 20,000 feet (6096 meters), 30,000 feet (9144 meters), and 40,000 feet (12,192 meters), respectively.

Climb Potential

The standard-day climb potential (or specific excess power) of the test airplane as determined from the level-flight acceleration data is presented in figures 9(a) to 9(e) for altitudes of 10,000 feet (3048 meters) to 50,000 feet (15,240 meters) at 10,000-foot (3048-meter) intervals. As expected, the variation of climb potential with increasing Mach number and altitude is similar to the trends of the curves of excess thrust presented in figure 6.

The relationship between excess thrust and climb potential, $(R/C)_S$, is given by the following rearranged version of equation (19) of the appendix:

$$(R/C)_S = \frac{(F_n - D)V_{T,s}}{W_s}$$

In the data analysis the gross weight, W_s, was a constant, and the climb potential is, therefore, directly proportional to the product of the excess thrust and true velocity, $V_{T,s}$, of the airplane. Thus, at a constant altitude the differences between the characteristics of the curves of climb potential presented in figure 9 and the curves of excess thrust presented in figure 6 are due to the effects of the true velocity on the climb potential.

The true velocity at a constant altitude is a linear function of Mach number. Its effect on the climb potential can be seen by comparing the excess-thrust and climb-potential data in figures 6(c) and 9(c), respectively. As shown, above Mach 1.0 the excess-thrust data remain fairly constant, though increasing slightly; whereas, the climb-potential data increase significantly because of the increasing value of the true velocity. Although present, the effects of true velocity on the climb-potential data are not as evident for altitudes of 20,000 feet (6096 meters), 40,000 feet (12,192 meters), and 50,000 feet (15,240 meters) as for 30,000 feet (9144 meters).

Comparison of Predicted and Flight-Test Data

In the initial phase of the test program, it was assumed that the predicted performance data would not represent the actual performance of the test airplane to the degree of accuracy required to compute meaningful flight trajectories. To evaluate this assumption, the predicted climb-potential data were computed and are presented in figure 9 as dashed lines. The data were computed from the standard F-104G performance characteristics (ref. 8) and do not include the effects of T_2 reset discussed previously.

For the predicted data to adequately represent the performance capability of the test airplane, it was believed that the difference between the predicted and test values of climb potential should not be greater than 10 percent at any point within the flight envelope. As shown in figure 9, the flight-test and predicted data do not agree within 10 percent over a significant portion of the flight envelope.

As a crosscheck of the level-acceleration data presented in figure 9, quasi-constant Mach number climbs were flown at the Mach numbers listed in table 2. The standard-day constant-Mach-number-climb performance data (climb potential and fuel-flow rate) presented in figures 10 and 11 were crossplotted in figures 8 and 9. The differences between the level-acceleration and climb data are attributed to the difficulty in establishing and holding the climb speed in the constant-Mach-number climbs because of the high climb rates encountered at the lower altitudes. As a result, the values of climb potential computed for the climb data are somewhat in error. These data are used, then, only for a qualitative crosscheck of the more accurate level-acceleration data.

Application of Flight-Test Results

The level-acceleration flight-test data presented in figure 9 were used to define a computer model in terms of excess thrust and fuel flow for the performance of the test airplane. This computer model was then used with the RUTowski OPtimization Computer Program (ref. 6) to generate a complete climb-potential map for the test airplane. This map, presented in figure 12, consists of lines of constant-climb potential plotted against true velocity and altitude. Figure 12 also presents a complete picture of the total performance capability of the test airplane.

The flight-test data and the data-analysis procedures used defined an accurate computer model for the computation of meaningful flight trajectories and provided a means of adjusting the performance model for variations in atmospheric conditions. But this information is still cumbersome to use in a real-time flight-path-optimization system because of the time required to compute and apply the correction factors to the performance model for the deviations in atmospheric conditions.

It would be highly desirable for a computer model to be defined in terms of the specific values of thrust and drag (that is, not just the difference between thrust and drag) for the entire flight envelope of an airplane. Then the correction factors required to adjust the performance model for variations in atmospheric conditions could be computed easily and applied directly to the values of thrust and drag. However, the large number of flight tests and the extensive instrumentation required to define such a model make this approach inefficient in terms of the cost and time required. Therefore, methods and techniques are needed for developing a computer model, in terms of thrust and drag, from test data so that data from a few flight tests can be used to define the performance for the entire flight envelope of any aircraft.

CONCLUDING REMARKS

A flight-test investigation was conducted to determine the performance characteristics of the F-104G, S/N 56-0790, airplane and to define a computer model for the performance of the airplane.

The climb-potential (specific excess power) data obtained from the flight tests were compared with available predicted performance data for the "average" or "typical" F-104G airplane. It was found that the predicted data did not represent the actual performance of the test airplane to the degree of accuracy required to compute meaningful flight trajectories. Therefore, the flight-test excess-thrust and fuel-flow data obtained were used to define an accurate performance model for the test airplane for a standard day at maximum afterburner power.

Even though the standardized flight-test data defined an accurate computer performance model, it would also be highly desirable for a computer model to be defined in terms of the specific values of thrust and drag for an entire flight envelope. However, the cost and time required for the large number of flight tests and the extensive instrumentation required to define such a model make this approach inefficient. Thus, there is a need for methods and techniques for developing a computer performance

model from test data so that data from a few flight tests can be used to define the performance for the entire flight envelope of an aircraft.

Flight Research Center,
National Aeronautics and Space Administration,
Edwards, Calif., January 29, 1971.

APPENDIX

DATA-ANALYSIS PROCEDURES

To correct the test-day data to standard-day conditions, a digital computer program was written to calculate the standard-day performance data from the level-flight-acceleration and constant-Mach-number-climb flight data, using specific-energy analysis methods of references 12 to 14. The procedure used to compute the standard-day data is outlined in the following discussion.

By using the flight-test-data input and the following equations, the standard-day climb-potential, excess-thrust, and fuel-flow data were computed for the test airplane for level-flight accelerations and constant-Mach-number climbs. The initial phase of the data analysis was the computation of the test-day performance of the airplane.

The indicated Mach number for each data point was determined from the values of indicated airspeed and indicated altitude corrected for instrumentation calibration errors as follows:

$$M_{ic} = f\left(V_{ic},\ h_{ic}\right) \tag{1}$$

The detailed equations for the calculation of the indicated Mach numbers are given in reference 12.

The true Mach number and true pressure altitude were determined from the indicated Mach number and the airspeed position-error curves (figs. 4 and 5) as follows:

$$M_T = M_{ic} + \Delta M_{pc} \tag{2}$$

$$h_{T,t} = h_{ic} + \Delta h_{pc} \tag{3}$$

The true test-day velocity, in knots, was then found by using the expression

$$V_{T,t} = 38.969 M_T \sqrt{T_{a,t}} \tag{4}$$

with $T_{a,t}$ obtained from the weather-balloon data in °C and changed to °K. The value of $V_{T,t}$ was changed to feet/second (meters/second), and the instantaneous specific energy for the airplane at the test-day conditions was determined by using the equation

$$He = h_{T,t} + \left(\frac{V_{T,t}^{\ 2}}{2g}\right) \tag{5}$$

The instantaneous value of climb potential at the test weight and thrust and with zero acceleration was obtained by determining the slope, at each test point, of a

smooth curve fitted to a time history of He as follows:

$$(R/C)_t = \frac{dHe}{dt} \tag{6}$$

The engine and afterburner fuel-used values for each data point were determined from the following equations:

$$FU_e = FC_e(K)\left(FD_e\right) \tag{7}$$

$$FU_{ab} = FC_{ab}(K)\left(FD_{ab}\right) \tag{8}$$

with the engine and afterburner fuel densities determined by

$$FD_e = FD_{es} + (K)\left(T_{f_{es}} - T_{f_e}\right)$$

$$FD_{ab} = FD_{es} + (K)\left(T_{f_{es}} - T_{f_{ab}}\right)$$

where K is a calibration constant.

The instantaneous total fuel used was then determined by using the expression

$$FU_{tot} = FU_e + FU_{ab} \tag{9}$$

The instantaneous airplane weight was determined by subtracting the total fuel used from the airplane weight at engine start as follows:

$$W_t = W_{t,es} - FU_{tot} \tag{10}$$

The instantaneous fuel flow was obtained by determining the slope, at each point, of a smooth curve fitted to the time history of the total fuel used for each data run, that is,

$$W_{f,t} = \frac{d\left(FU_{tot}\right)}{dt} \tag{11}$$

After the test-day data were computed, the following equations were used to correct

the test data to the selected standard-day conditions. Corrections were applied for the nonstandard-day temperature effects on the altitude, true airspeed, thrust, and fuel flow and for the nonstandard weight effects on the airplane's inertial and induced drag.

For a given level-flight acceleration, the selected test altitude was the altitude to which the data were standardized. The standard-day temperature and pressure were then computed for the selected standard altitude as follows:

$$T_{a,s} = f\left(h_{T,s}\right) \tag{12}$$

$$p_{a,s} = f\left(h_{T,s}\right) \tag{13}$$

The exact equations used to compute these quantities are given in reference 12. For the constant-Mach-number-climb data, $T_{a,s}$ and $p_{a,s}$ were computed as a function of $h_{T,t}$. The standard-day true velocity, $V_{t,s}$, in knots, was then calculated from equation (4) substituting $T_{a,s}$ for $T_{a,t}$.

The change in thrust, ΔF_n, resulting from nonstandard-day temperatures was obtained from a plot of $\dfrac{\dfrac{\Delta F_n}{\delta_{t_2}}}{T_{T,s} - T_{T,t}}$ versus test-day total temperature. The data for this plot were obtained from reference 8. The change in thrust was then computed as follows:

$$\Delta F_n = \frac{\dfrac{\Delta F_n}{\delta_{t_2}}}{T_{T,s} - T_{T,t}} \left(T_{T,s} - T_{T,t}\right)\left(\delta_{t_2}\right) \tag{14}$$

The correction to the test-day climb potential for the nonstandard-day temperature effects on thrust, $\Delta(R/C)_{power}$, was then determined by using the equation

$$\Delta(R/C)_{power} = \frac{\left(\Delta F_n\right)(101.33)\left(V_{T,s}\right)}{W_t} \tag{15}$$

Corrections were then applied to correct the test-day airplane weight to a standard weight. The weight correction was divided into two portions. The first portion was the inertia correction, $\Delta(R/C)_w$, and was determined with the expression

$$\Delta(R/C)_W = \left[(R/C)_t \sqrt{\frac{T_{a,t}}{T_{a,s}}} + \Delta(R/C)_{power}\right]\left(\frac{W_t - W_s}{W_s}\right) \tag{16}$$

It should be noted that the temperature corrections for true velocity and geometric altitude for a constant test-day Mach number are included in $\frac{T_{a,t}}{T_{a,s}}$. The second portion of the weight correction was the induced-drag correction, $\Delta(R/C)_{id}$, which was determined as follows:

$$\Delta(R/C)_{id} = \frac{\left(\Delta C_{D_{id}}\right)\left(q_t\right)(S)\left(V_{T,t}\right)}{W_t} \tag{17}$$

where

$$\Delta C_{D_{id}} = \frac{\Delta C_D}{\Delta C_L{}^2}\left(C_{L_t}{}^2 - C_{L_s}{}^2\right)$$

which is the change in the induced-drag coefficient. Combining the above corrections, the standard-day climb potential was determined by

$$(R/C)_s = (R/C)_t \sqrt{\frac{T_{a,t}}{T_{a,s}}} + \Delta(R/C)_{power} + \Delta(R/C)_W + \Delta(R/C)_{id} \tag{18}$$

The value of $V_{T,s}$ was changed to feet/minute (meters/second), and the standard-day excess thrust was computed by

$$F_{n,ex} = \frac{(R/C)_s\left(W_s\right)}{V_{T,s}} \tag{19}$$

The change in fuel flow, ΔW_f, for nonstandard-day temperatures was determined from a plot of $\frac{\frac{\Delta W_f}{\delta_{t_2}}}{T_{T,s} - T_{T,t}}$ versus the test-day total temperature. The data for the plot were obtained from reference 8. The change in fuel flow is then computed as follows:

$$\Delta W_f = \frac{\dfrac{\Delta W_f}{\delta_{t_2}}}{T_{T,s} - T_{T,t}} \left(T_{T,s} - T_{T,t}\right)\left(\delta_{t_2}\right) \tag{20}$$

The fuel flow was then corrected to the standard-day conditions by using the expression

$$W_{f,s} = \left(W_{f,t} + \Delta W_f\right)\left(\frac{p_{a,s}}{p_{a,t}}\right) \tag{21}$$

For the level-flight acceleration data the values of $(R/C)_s$, $F_{n,ex}$, and $W_{f,s}$ were plotted against Mach number for each of the selected standard-day altitudes. For the climb data the values of $(R/C)_s$, $W_{f,s}$, and $M_{T,t}$ were plotted against altitude for each climb schedule flown.

REFERENCES

1. Bryson, A. E.; and Denham, W. F.: A Steepest-Ascent Method for Solving Optimum Programming Problems. J. Appl. Mech., vol. 29, series E, no. 2, June 1962, pp. 247-257.

2. Stein, Lawrence H.; Matthews, Malcolm L.; and Frenk, Joel W.: STOP - A Computer Program for Supersonic Transport Trajectory Optimization. The Boeing Co. (NASA CR-793), 1967.

3. Mobley, R. L.; and Vorwald, R. F.: Three-Degree-of Freedom Problem Optimization Formulation. Volume 3. User's Manual. Tech. Doc. Rep. No. FDL-TDR-64-1, Part II, Volume 3, Air Force Flight Dynamics Lab., Wright-Patterson Air Force Base, Ohio, June 1964.

4. Schmidt, H. E.; Helgason, R. V.; Witherspoon, J. T.; and Geib, K. E.: Trajectory Optimization by Method of Steepest Descent. Volume III Programmer's Manual. Tech. Rep. AFFDL-TR-67-108, Air Force Flight Dynamics Lab., Wright-Patterson Air Force Base, Ohio, April 1968.

5. Lamb, George H.: Validation of the Energy-Maneuverability Theory - Optimum Flight Path for the F-4C Aircraft. Tech. Rep. APGC-TR-66-27, Air Proving Ground Center, Eglin Air Force Base, Fla., April 1966.

6. Porter, Milton B., Jr.: RUTOP-Rutowski Optimization Computer Program. Tech. Rep. FTC-TR-68-14, Air Force Flight Test Center, Edwards Air Force Base, Calif., Jan. 1969.

7. Bellman, Richard; and Kalaba, Robert: Dynamic Programming and Modern Control Theory. Academic Press Inc., N. Y., c. 1965.

8. Avant, N. J.: Performance Characteristics - Appendix A. Rep. No. 16097 App. A, Lockheed Aircraft Corp., July 16, 1962.

9. Mechtly, E. A.: The International System of Units - Physical Constants and Conversion Factors. NASA SP-7012, 1969.

10. Michaels, J. M.; Wesling, G. C.; Housley, F. R.; and Henderson, R. L.: J79-GE-7, J79-GE-11, J79-GE-11A Turbojet Engine. R60FPD451. Flight Propulsion Div., General Electric, Sept. 1960.

11. Richardson, Norman R.; Pearson, Albin O.: Wind-Tunnel Calibrations of a Combined Pitot-Static Tube, Vane-Type Flow-Direction Transmitter, and Stagnation-Temperature Element at Mach Numbers From 0.60 to 2.87. NASA TN D-122, 1959.

12. Herrington, Russel M.; Shoemacher, Paul E.; Bartlett, Eugene P.; and Dunlap, Everett W.: Flight Test Engineering Handbook. Tech. Rep. No. 6273, Air Force Flight Test Center, May 1951 (rev. Jan. 1966).

13. Godwin, O. D.; Frazier, F. D.; and Durnin, R. E.: Performance Flight Test Techniques. FTC-TIH 64-2006, USAF Aerospace Research Pilot School, Edwards Air Force Base, Calif.

14. Hendrix, George D.; Godwin, Orgle D.; Frazier, Frank D.; and Durnin, Rodney E.: Performance Flight Testing Theory. FTC-TIH 64-2005, USAF Aerospace Research Pilot School, Edwards Air Force Base, Calif.

15. Anon.: Flight Manual F/RF/TF-104G. T. O. 1F-104G-1, U. S. Air Force, pp. 1-12 (rev. July 1968), pp. 6-11 (rev. Oct. 1967).

TABLE 1.-PERTINENT PHYSICAL CHARACTERISTICS OF THE TEST AIRPLANE

General:	
Length, ft (m)	54.77 (16.69)
Height, ft (m)	13.49 (4.11)
Wing:	
Area, ft^2 (m^2)	196.1 (18.2)
Span, ft (m)	21.94 (6.69)
Aspect ratio	2.45
Fuselage:	
Frontal area, ft^2 (m^2)	25.00 (2.3)
Length, ft (m)	51.25 (15.62)
Fineness ratio	9.09
Horizontal tail:	
Area, ft^2 (m^2)	48.2 (4.5)
Span, ft (m)	11.91 (3.63)
Aspect ratio	2.95
Deflection, deg (rad)	5 to -17 (0.087 to -0.297)
Weight:	
Basic, lb (kg)	13,608 (6172)
Pilot, lb (kg)	230 (104)
Fuel, lb (kg)	6228 (2825)
Total, lb (kg)	20,066 (9102)

TABLE 2.-FLIGHT-TEST CONDITIONS

Flight conditions	Power	Test runs	Altitude, ft (m)	Mach range
Level acceleration	Maximum after-burner	2	10,000 (3048)	0.5 to 1.2
		2	20,000 (6096)	0.6 to 1.6
		2	30,000 (9144)	0.6 to 1.9
		2	40,000 (12,192)	0.8 to 2.0
		2	50,000 (15,240)	1.4 to 2.0
Constant-Mach-number climb	Maximum after-burner	2	5000 (1524) to ceiling	0.6
		1	5000 (1524) to ceiling	0.7
		2	5000 (1524) to ceiling	0.75
		2	5000 (1524) to ceiling	0.90
		1	30,000 (9144) to ceiling	1.5
		1	30,000 (9144) to ceiling	1.85
		1	35,000 (10,668) to ceiling	1.95

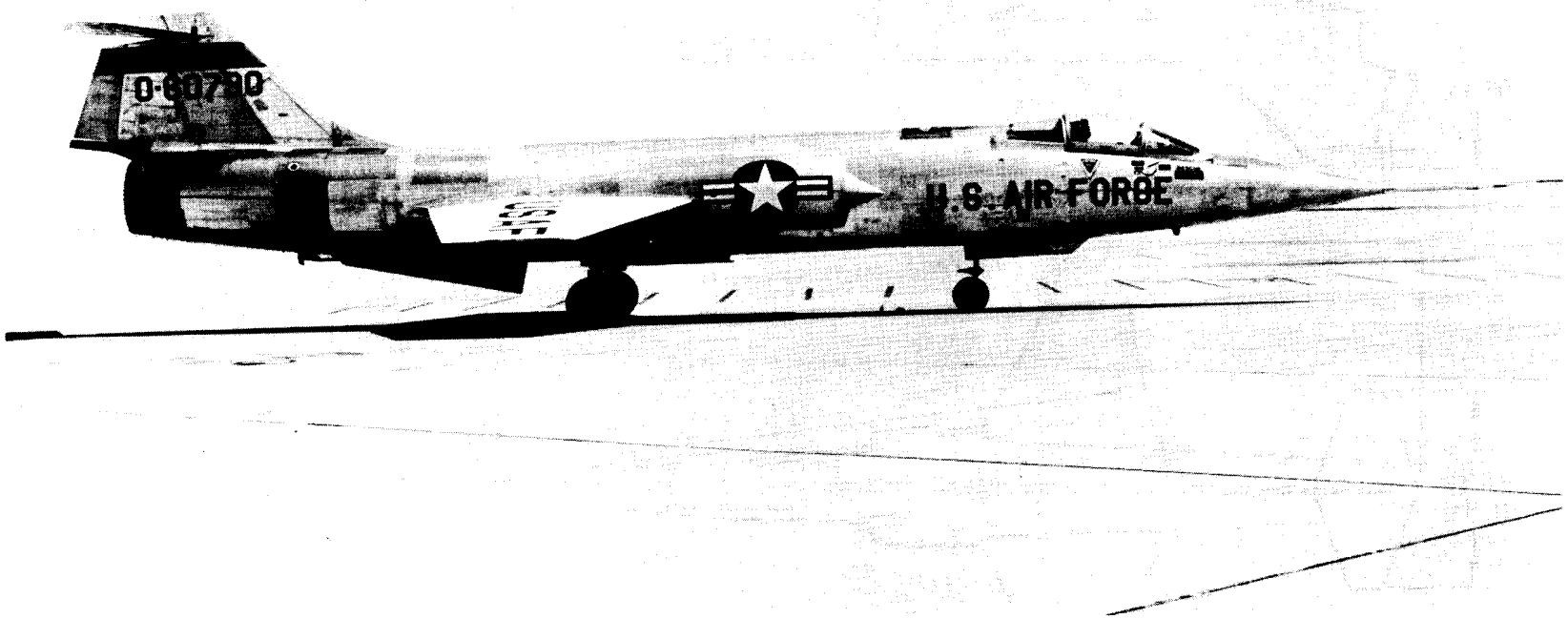

Figure 1. F-104G, S/N 56-0790, test airplane.

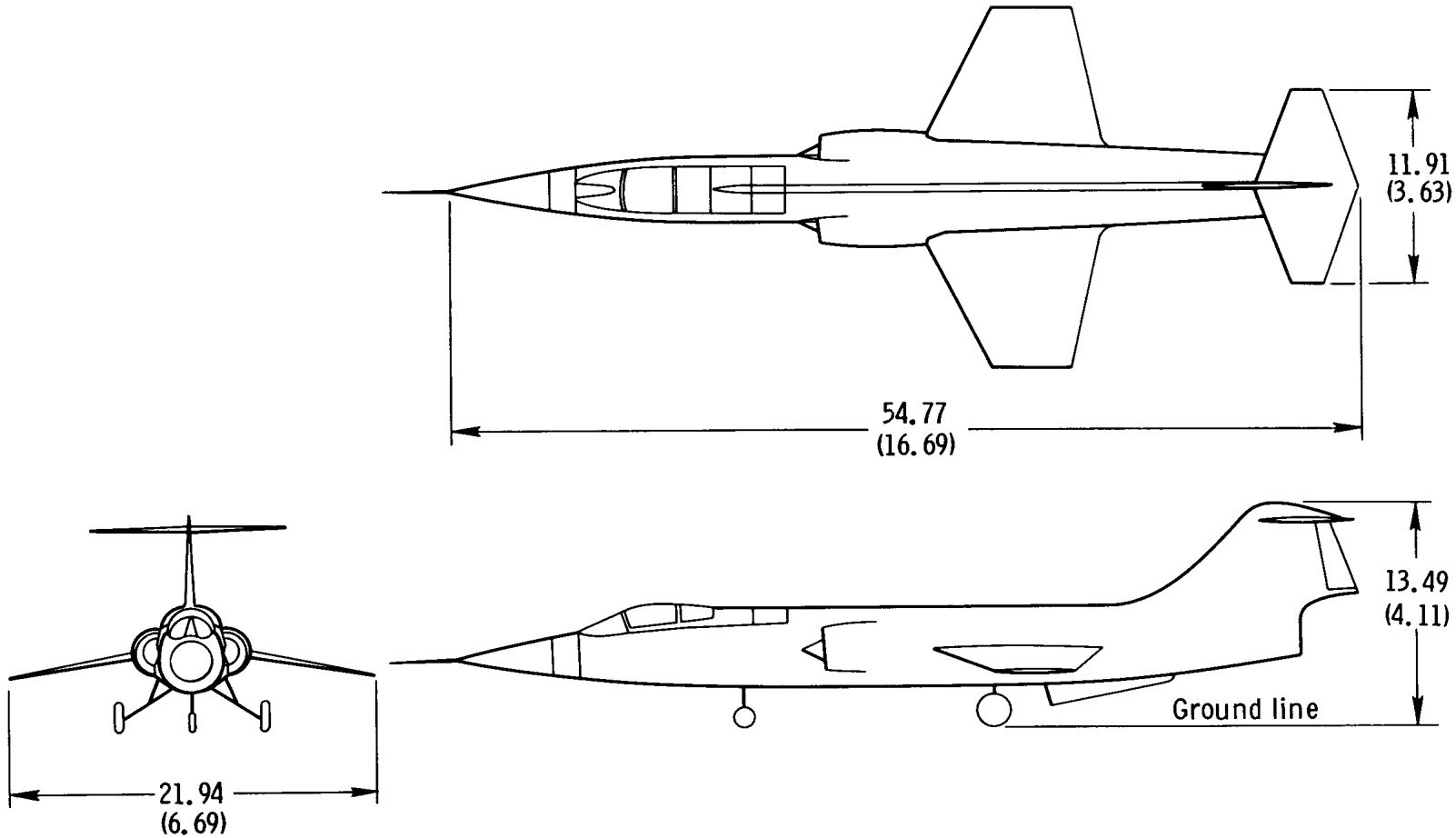

Figure 2. Three-view drawing of the F-104G airplane. Dimensions in feet (meters).

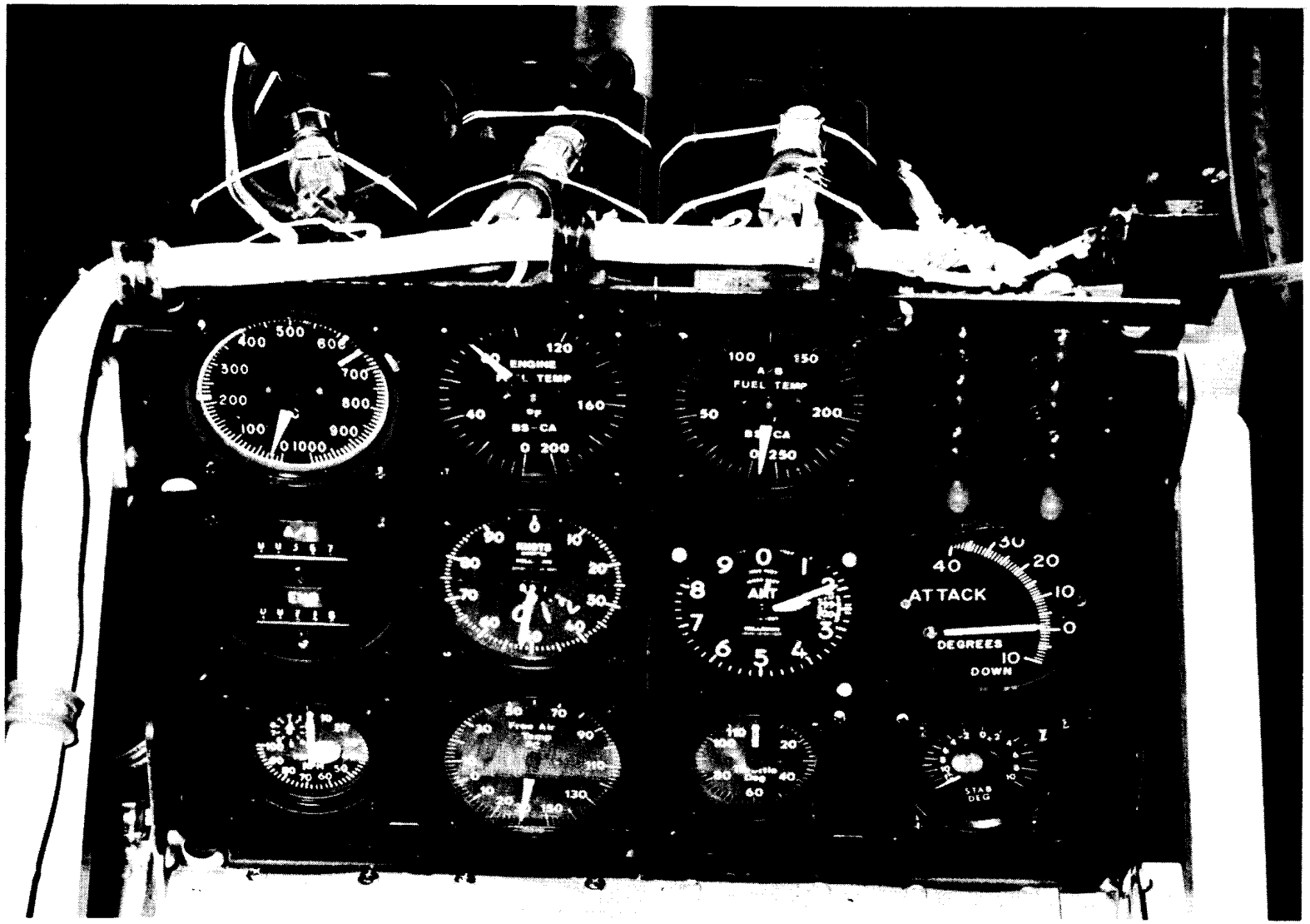

Figure 3. Photopanel installed in test airplane. E-19582

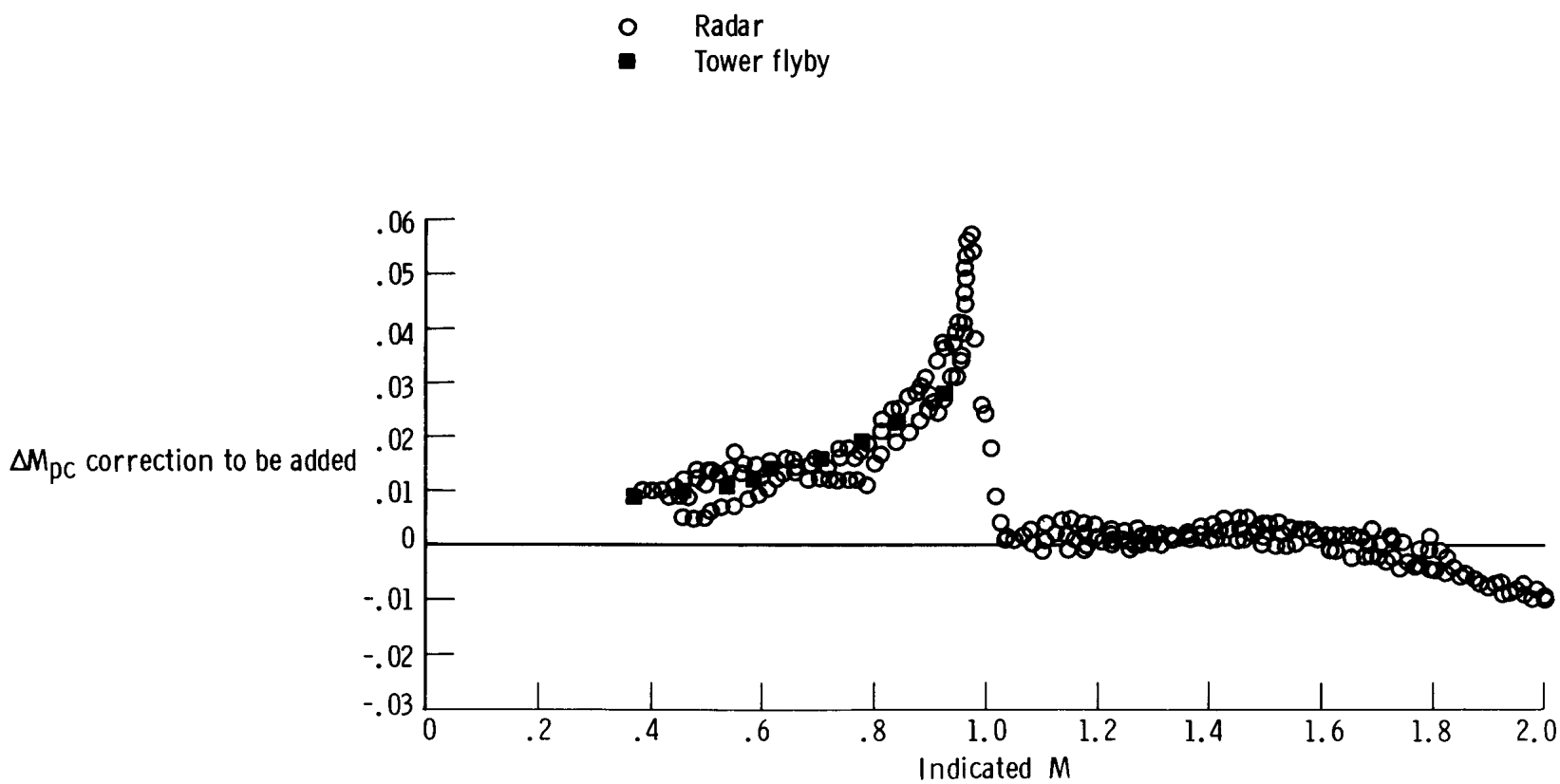

Figure 4. Position-error calibration for Mach number.

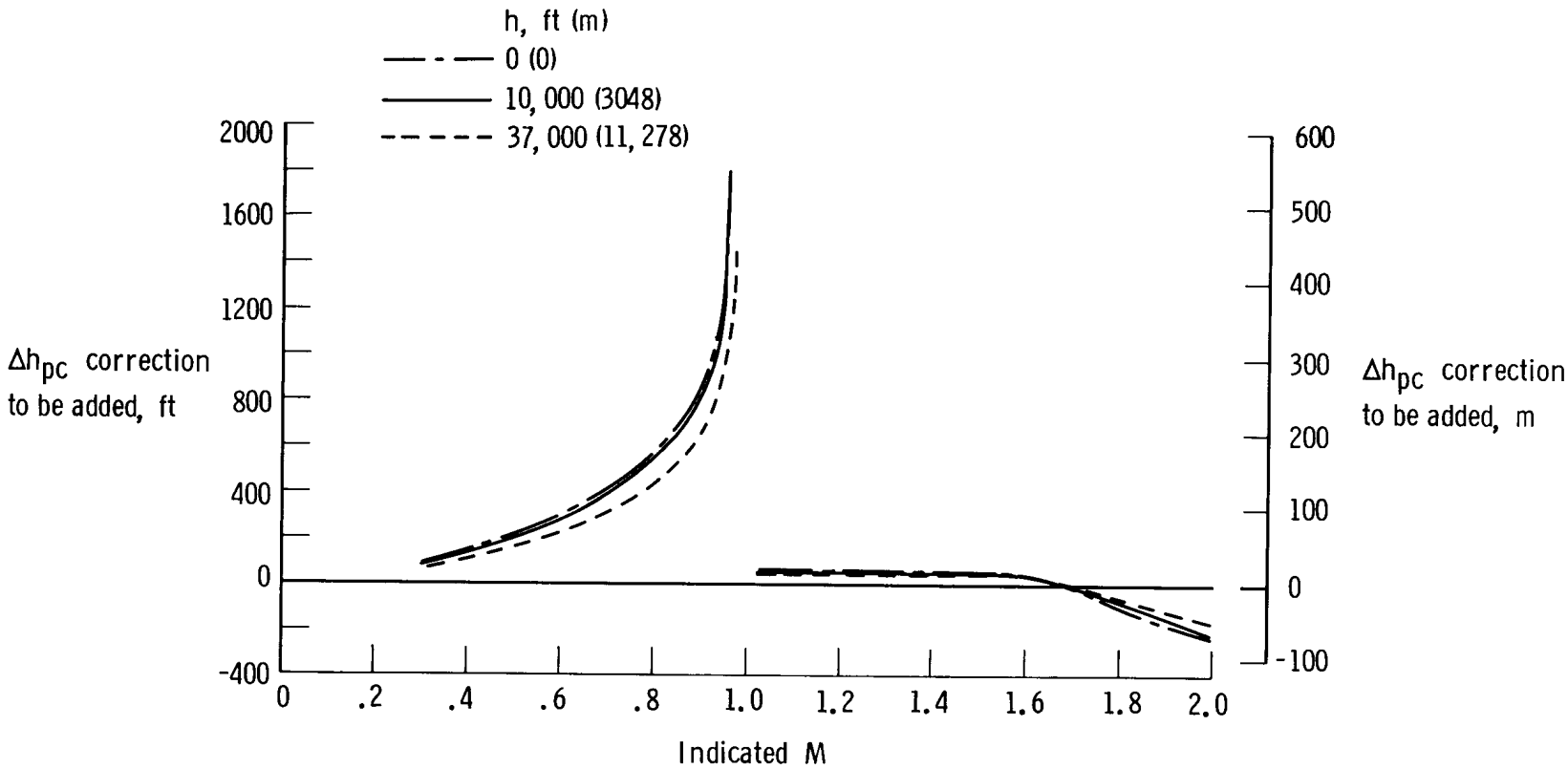

Figure 5. Position-error calibration for altitude.

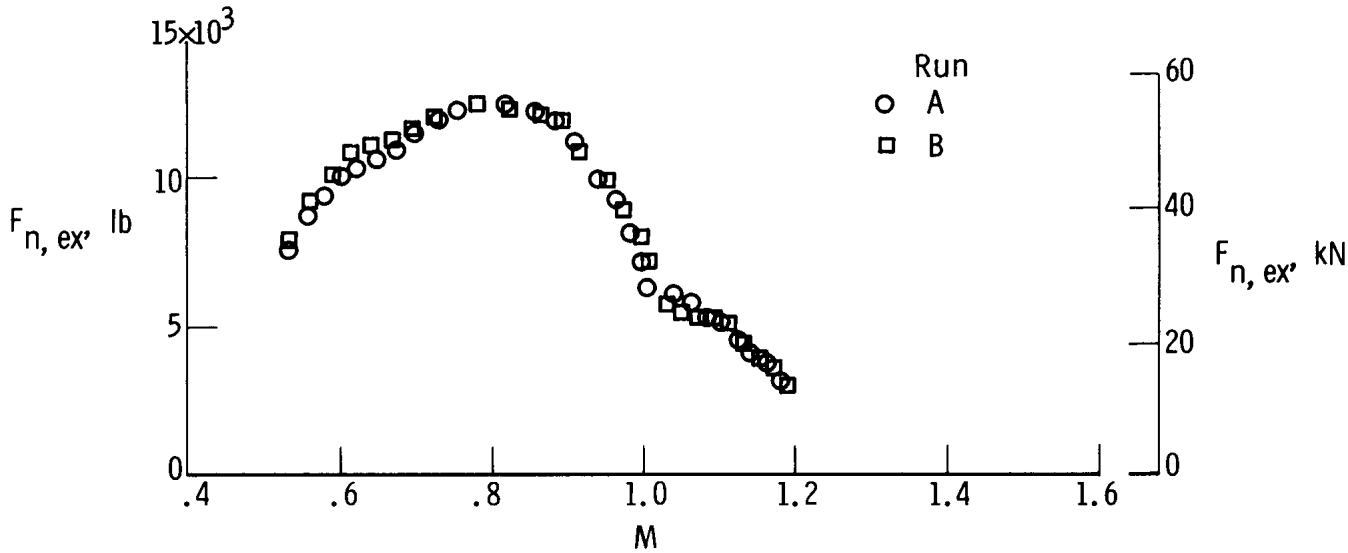

(a) Altitude = 10,000 ft (3048 m).

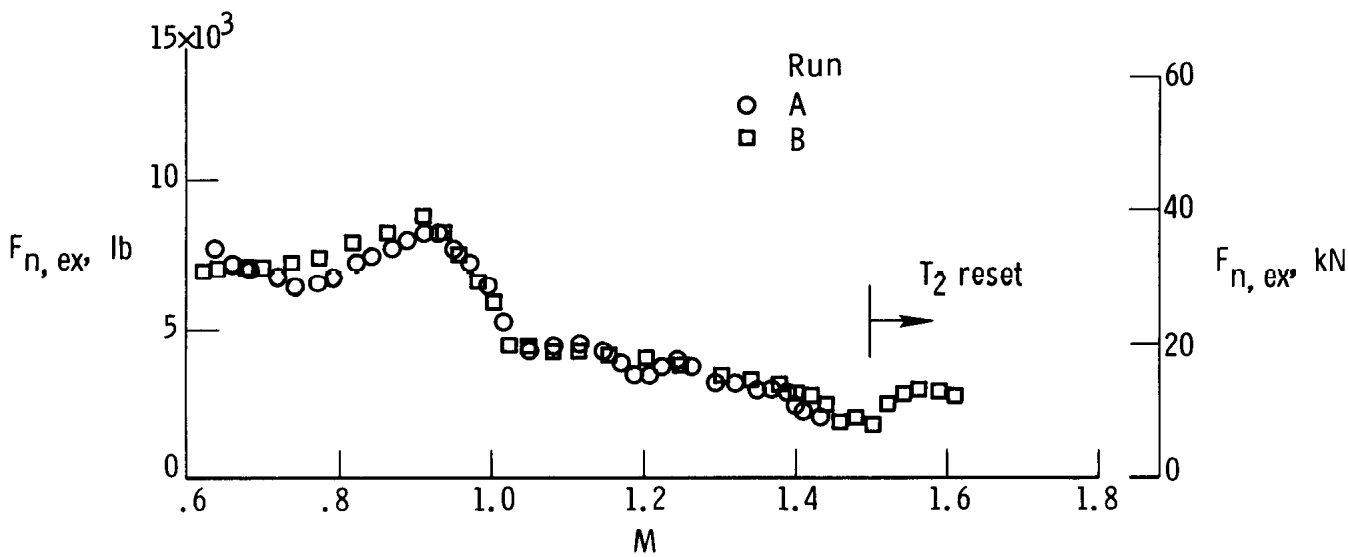

(b) Altitude = 20,000 ft (6096 m).

Figure 6. Standard-day excess thrust for the test airplane obtained from flight at a normal load factor of 1, maximum afterburner power, gross weight of 18,000 pounds (8165 kilograms), and with no external stores.

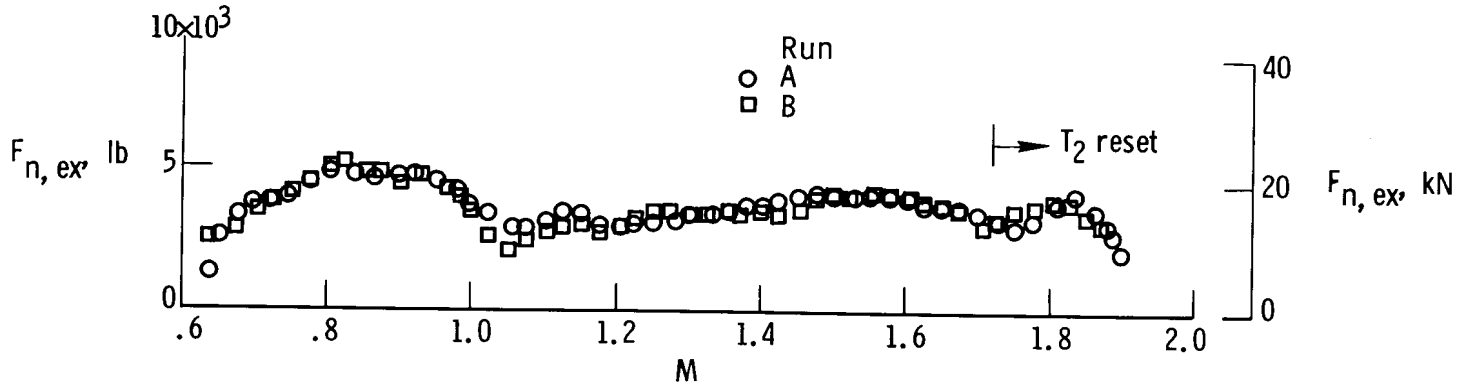

(c) Altitude = 30,000 ft (9144 m).

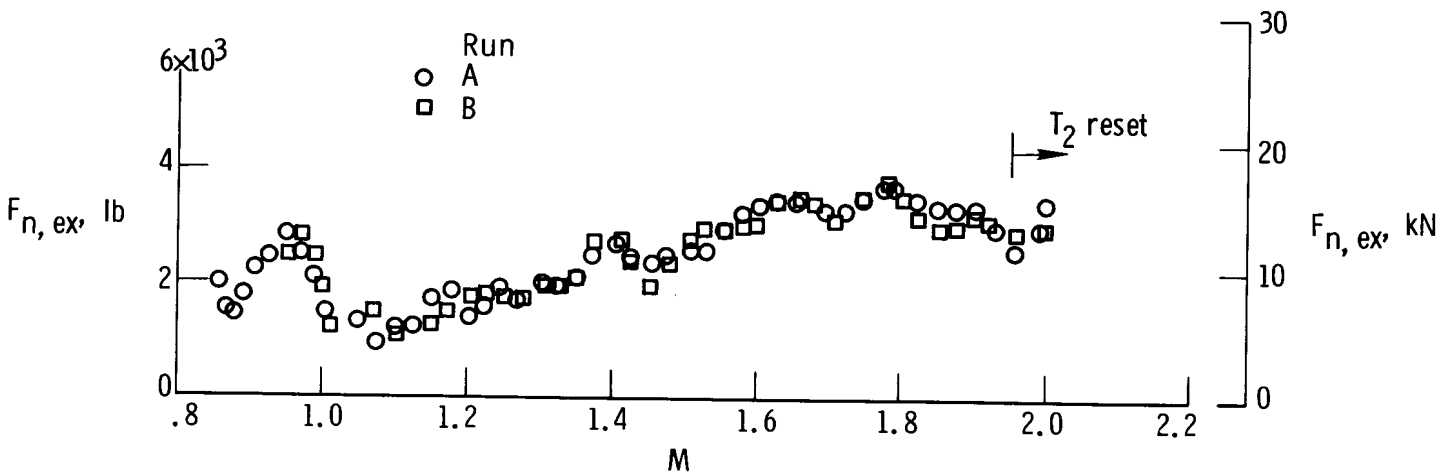

(d) Altitude = 40,000 ft (12,192 m).

Figure 6. Continued.

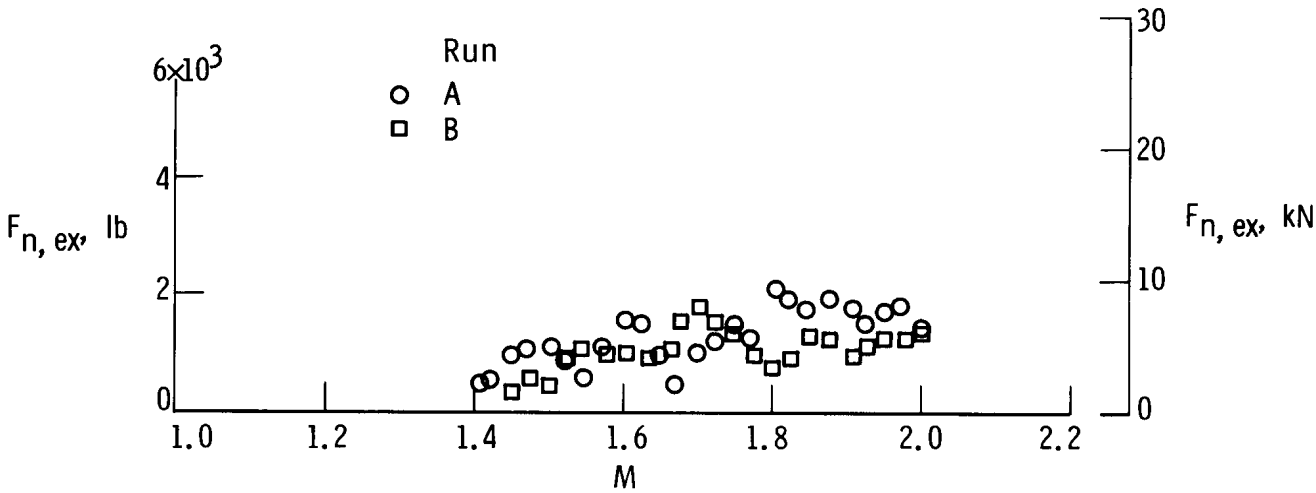

(e) Altitude = 50,000 ft (15,240 m).

Figure 6. Concluded.

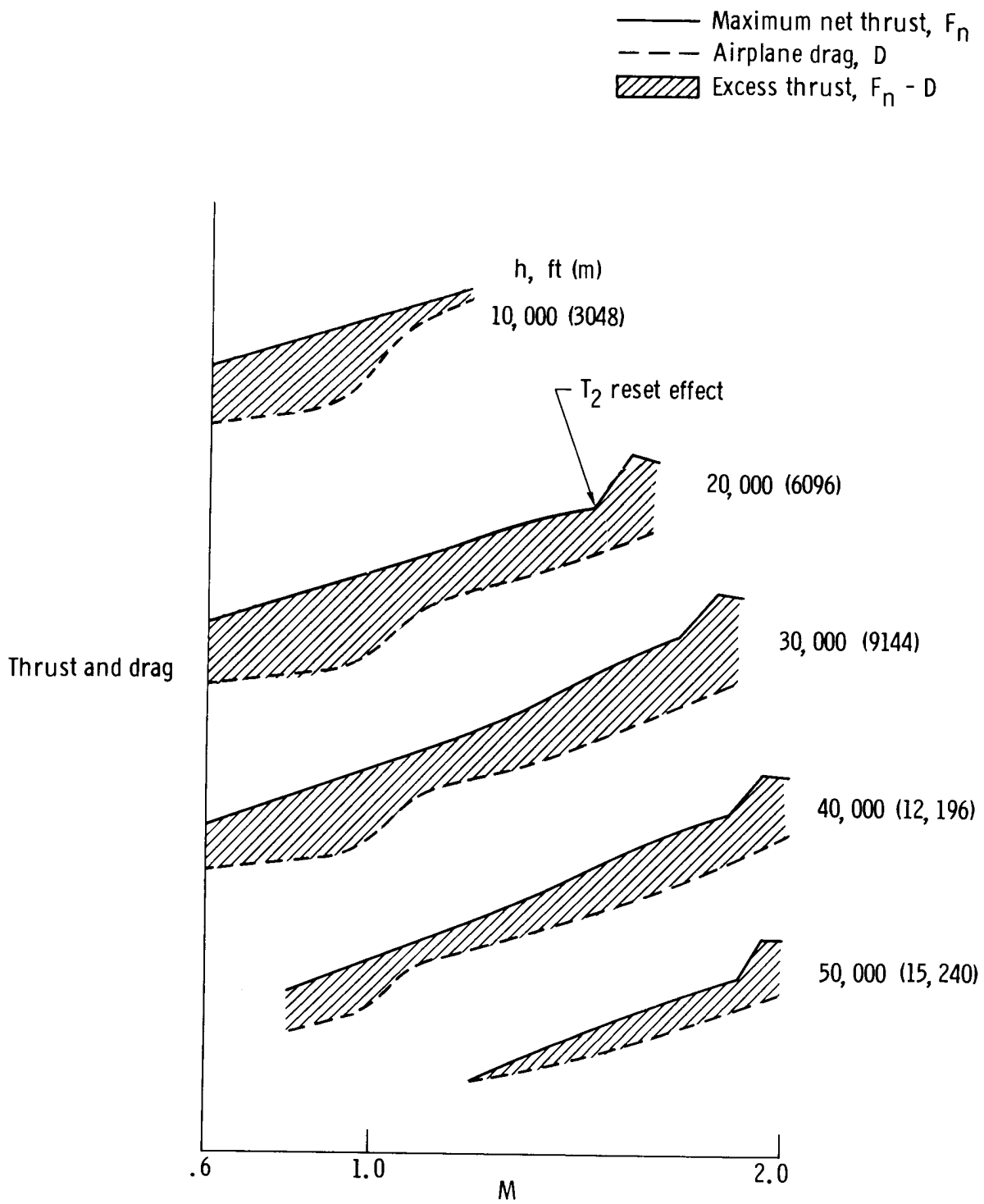

Figure 7. Schematic of typical thrust and drag curves (ref. 15) for the test airplane at maximum afterburner power and constant gross weight.

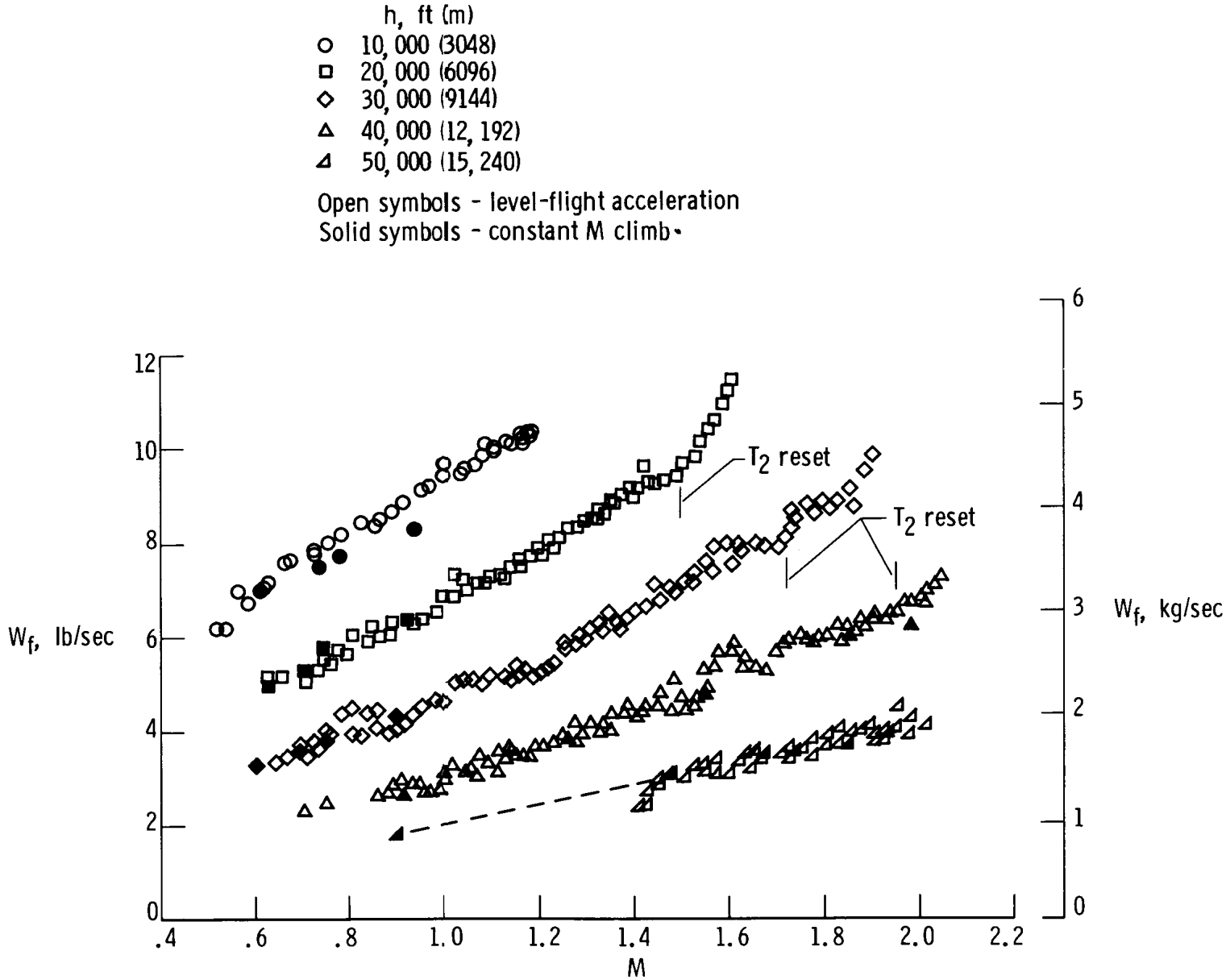

Figure 8. Standard-day fuel flow for the J79-GE-11A engine installed in the test airplane at maximum afterburner power.

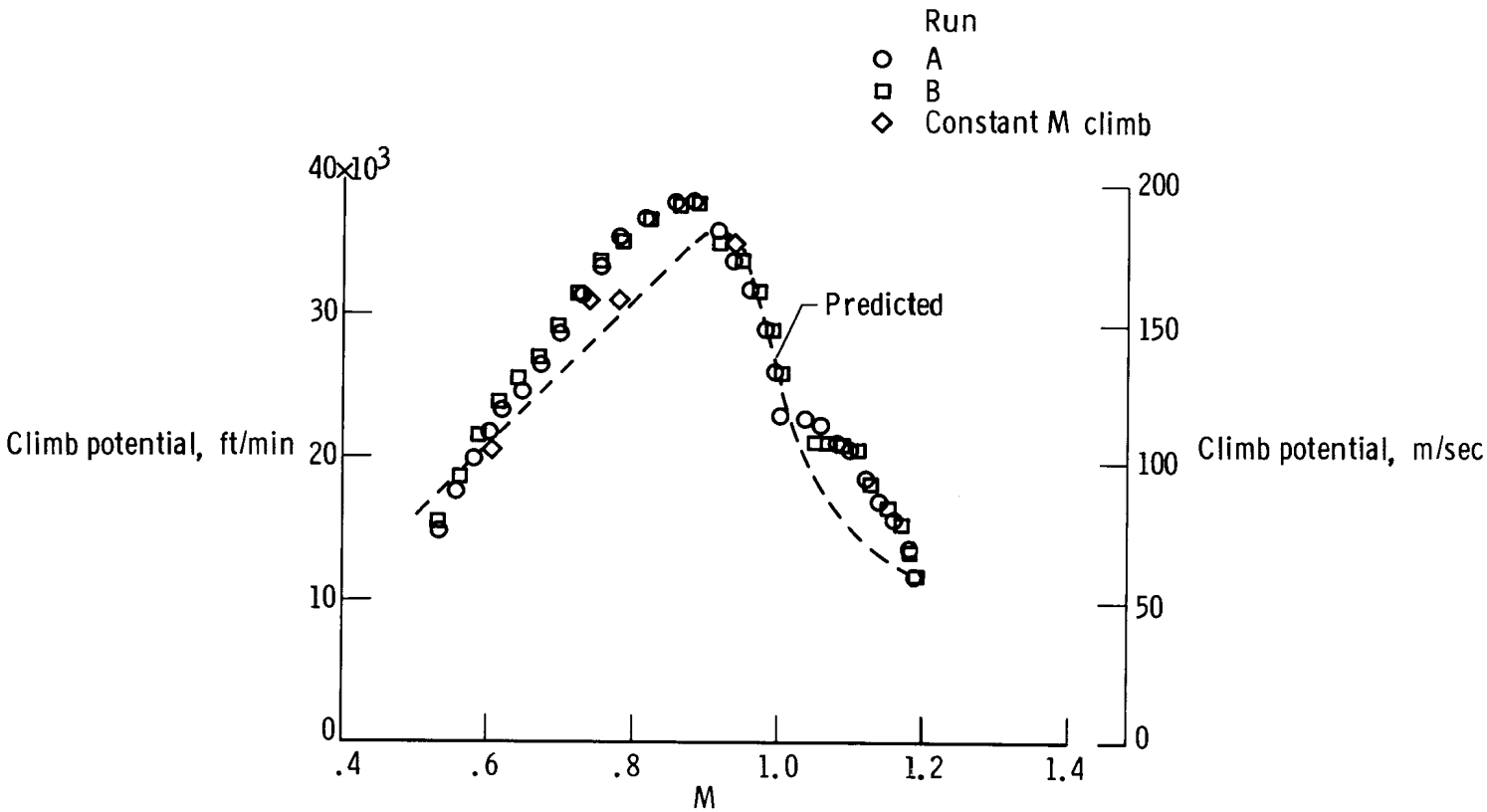

(a) Altitude = 10,000 ft (3048 m).

Figure 9. Standard-day climb potential for the test airplane obtained from level-flight accelerations at a normal load factor of 1, maximum afterburner power, gross weight of 18,000 pounds (8165 kilograms), and with no external stores.

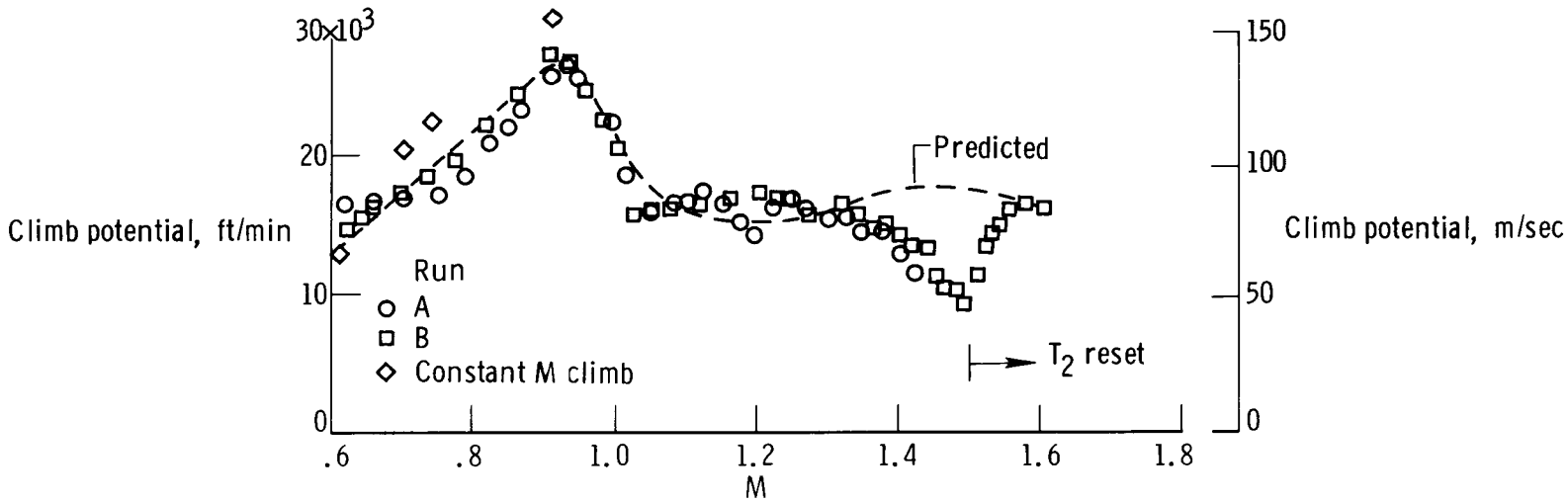

(b) Altitude = 20,000 ft (6096 m).

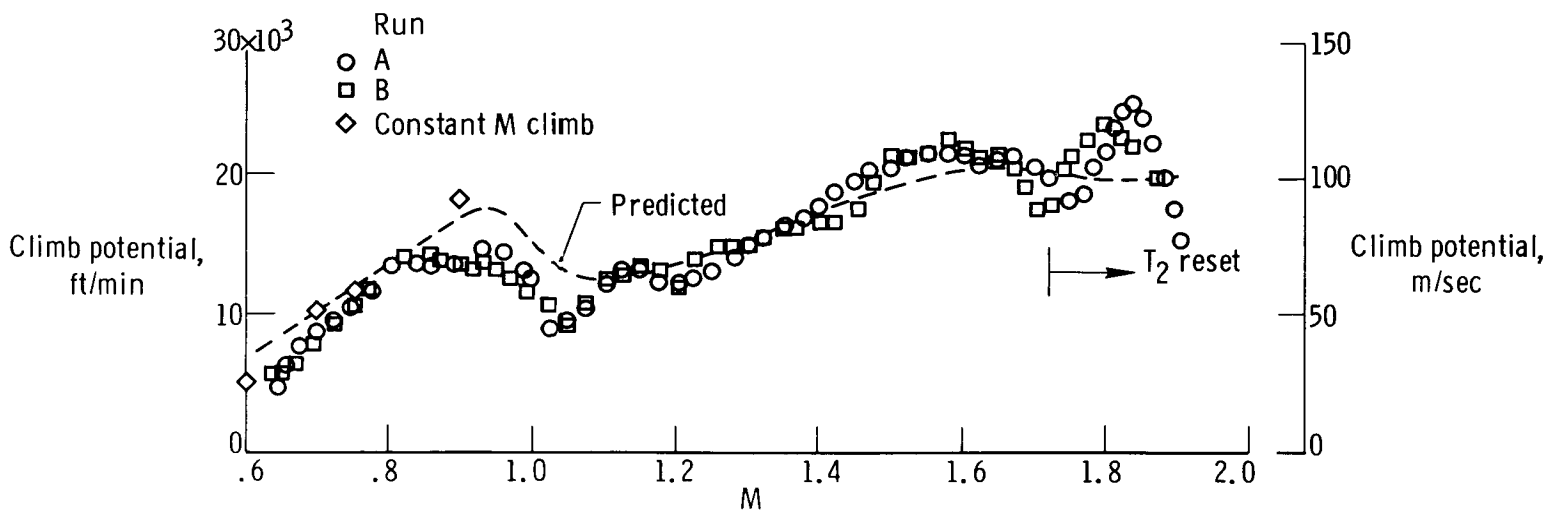

(c) Altitude = 30,000 ft (9144 m).

Figure 9. Continued.

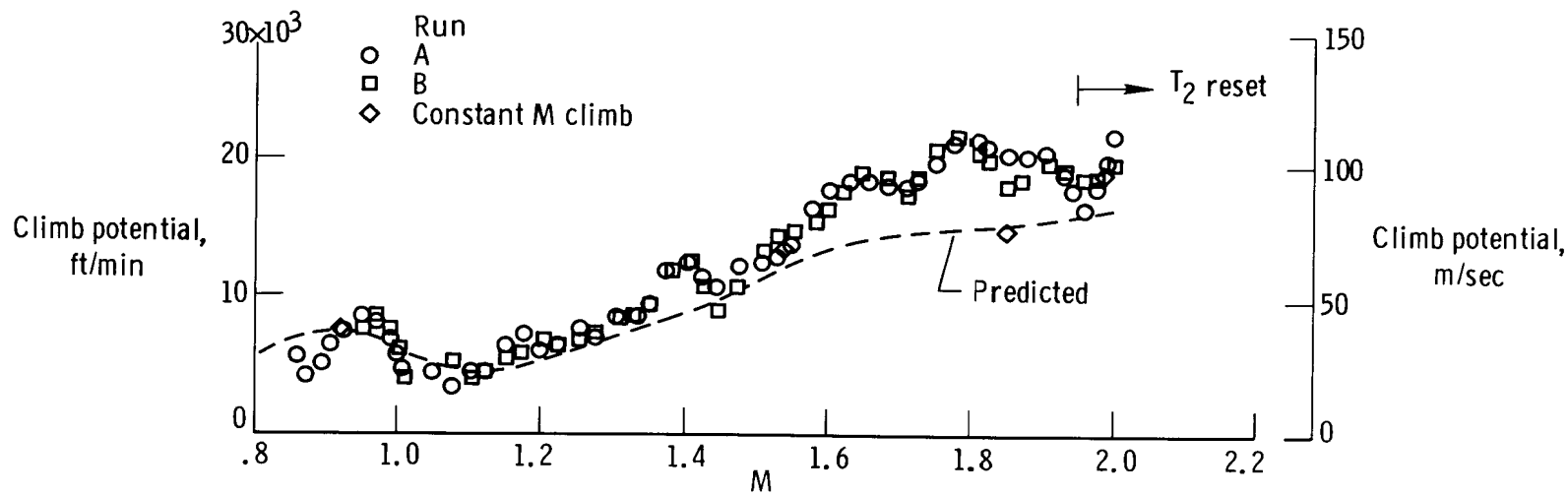

(d) Altitude = 40,000 ft (12,192 m).

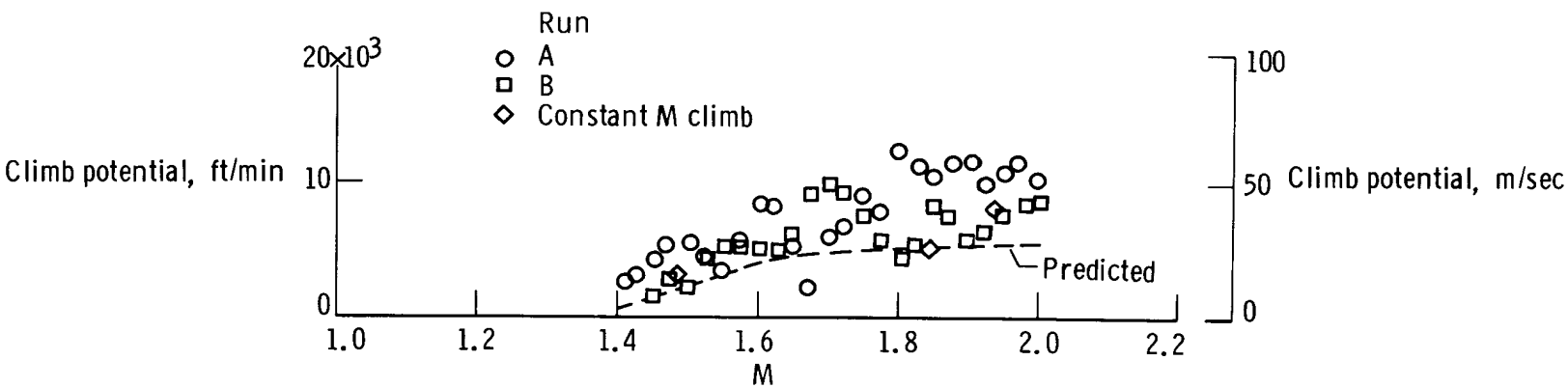

(e) Altitude = 50,000 ft (15,240 m)

Figure 9. Concluded.

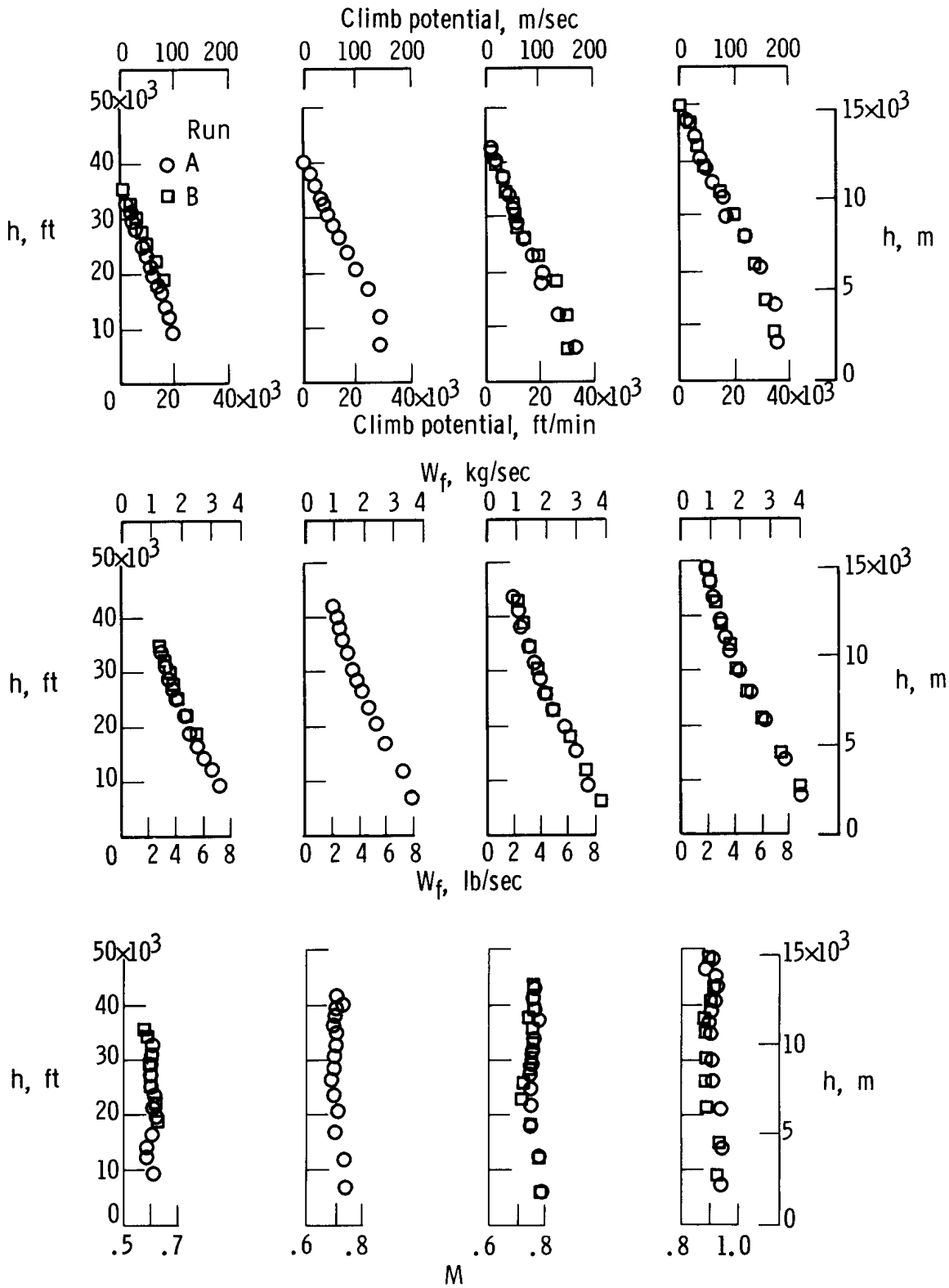

Figure 10. Standard-day subsonic climb performance of the test airplane at a normal load factor of 1, maximum afterburner power, gross weight of 18,000 pounds (8165 kilograms), and with no external stores.

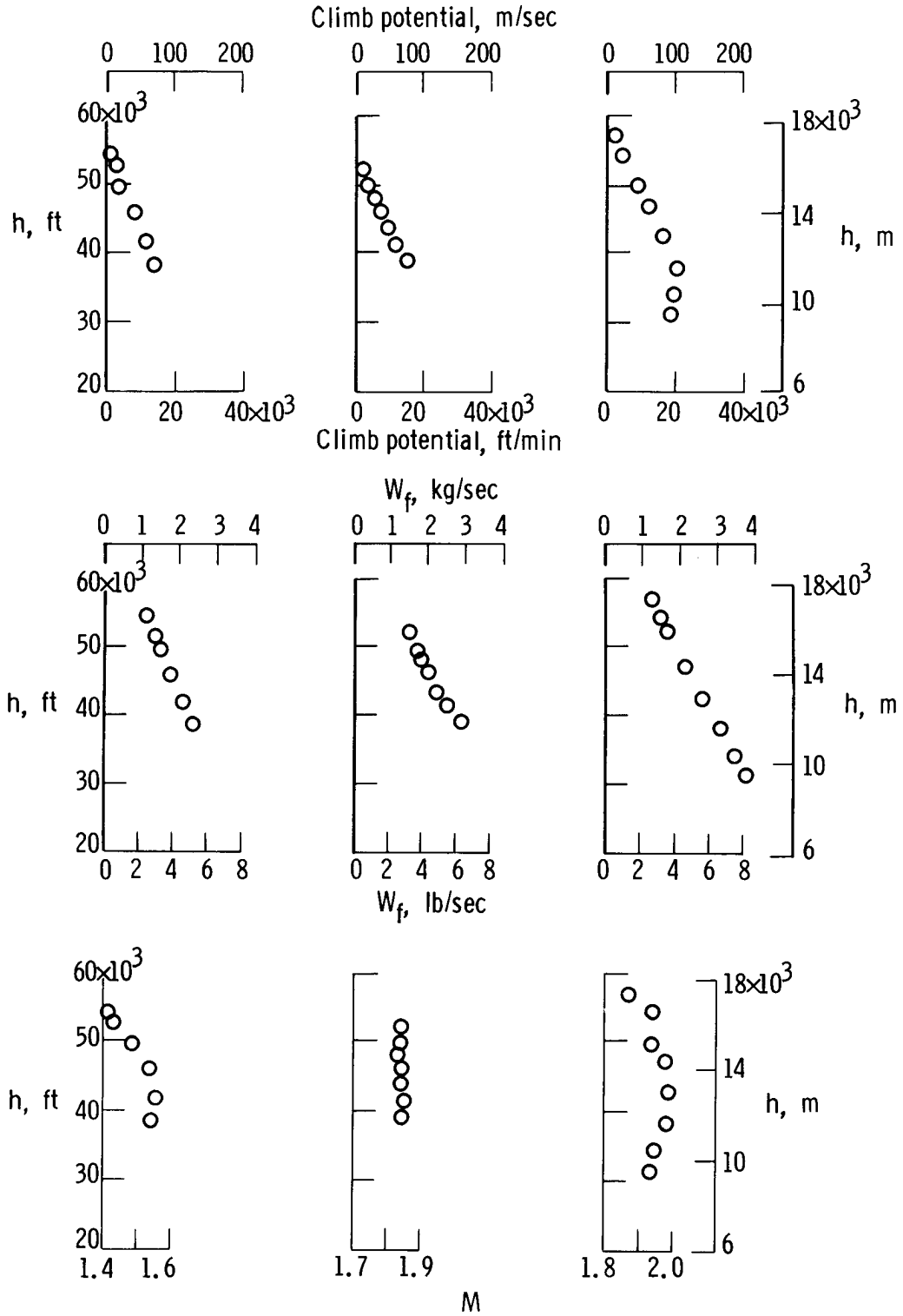

Figure 11. Standard-day supersonic climb performance of the test airplane at a normal load factor of 1, maximum afterburner power, gross weight of 18,000 pounds (8165 kilograms), and with no external stores.

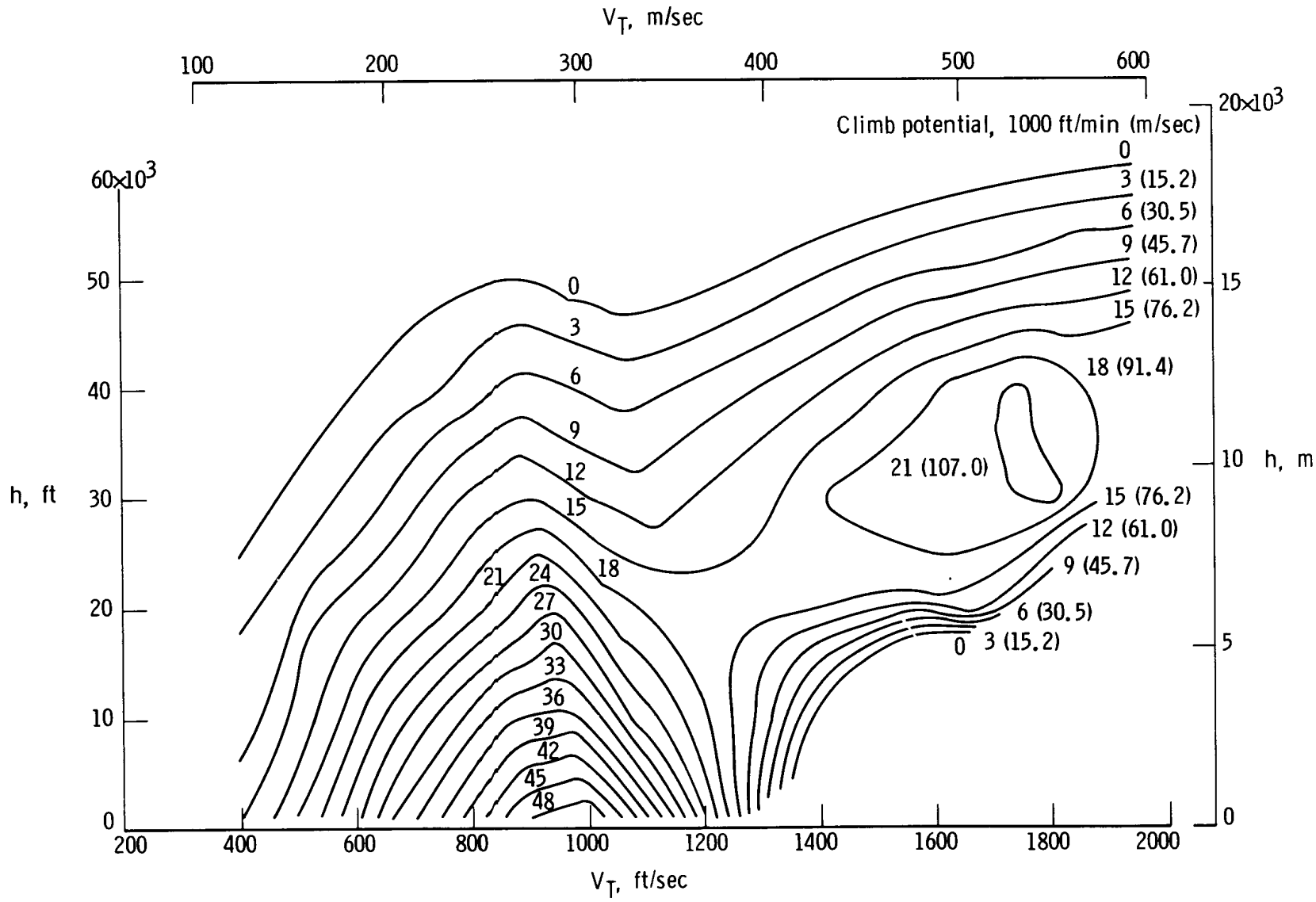

Figure 12. F-104, S/N 790, standard-day climb-potential contours derived from flight at a normal load factor of 1, maximum afterburner power, and a gross weight of 18,000 pounds (8165 kilograms).

NASA-Langley, 1971 — 2 H-636